Synthesis of Diiron μ-Allenyl Complexes by Electrophilic Addition to Propen-2-yl-Dimetallacyclopentenone Species: a Joint Experimental and DFT Study

Gabriele Agonigi,[a] Marco Bortoluzzi,[b] Tiziana Funaioli,[a] Fabio Marchetti,*[,a] Guido Pampaloni,[a] Stefano Zacchini [c]

[a] *Dipartimento di Chimica e Chimica Industriale, University of Pisa, Via Risorgimento 35, 56126 Pisa (I).*

[b] *Dipartimento di Scienze Molecolari e Nanosistemi, University of Venezia, Dorsoduro 2137, I-30123 Venezia, Italy.*

[c] *Dipartimento di Chimica Industriale "Toso Montanari", University of Bologna, Viale Risorgimento 4, I-40136 Bologna.*

Received.....; accepted ……

*Corresponding author: Dr. Fabio Marchetti.

Tel.: *int. code* 0502219245; E-mail address: fabmar@dcci.unipi.it

Webpage: http://www.dcci.unipi.it/~fabmar/

Abstract

The propen-2-yl-dimetallacyclopentenone complex [$Fe_2Cp_2(CO)(\mu\text{-}CO)\{\mu\text{-}\eta^1{:}\eta^3\text{-}C_\alpha(H)=C_\beta(C_\gamma(CH_3)CH_2)C(=O)\}$] (**1**) underwent electrophilic additions at the propenyl moiety to afford the μ-allenyl complexes [$Fe_2Cp_2(CO)_2(\mu\text{-}CO)\{\mu\text{-}\eta^1{:}\eta^2{}_{\alpha,\beta}\text{-}C_\alpha H=C_\beta=C_\gamma(CH_3)(CH_2E)\}][BF_4]$ (E = CPh_3, [**2**][BF_4]; E = H, [**3**][BF_4]), in ca. 85% yield. The molecular structure of ([**2**][BF_4]) was ascertained by X-ray diffractometry; X-ray, NMR and DFT results agreed in that one single isomer formed, bearing the [CH_2CPh_3] group pointing far from the Fe–Fe axis. The reaction of [**3**][BF_4] with $NHEt_2$ in the presence of PhSSPh resulted in the prevalent formation of [$FeCp(CO)_2SPh$] (**7**).

Keywords: diiron complexes, allenyl ligand, propen-2-yl-dimetallacyclopentenone, C–C bond formation, electrochemistry, DFT calculations.

1. Introduction

Dinuclear complexes endow a variety of reactivity patterns to bridging hydrocarbyl ligands and offer the possibility of stabilizing coordination modes, as consequence of the cooperativity of the two metal centres working in concert [1]. In this context, the reactivity of diiron complexes based on the [$Fe_2Cp_2(CO)(\mu\text{-}CO)$] core has aroused increasing attention in the last years due to the interest in the preparation of functionalized organic fragments, that cannot be easily achieved through conventional organic protocols, by assistance of non toxic metal centres [2]. In general, allenyl ligands bridged-coordinated to di- or polynuclear systems have proved to be feasible materials for the formation of unusual metallorganic species [3]. Several synthetic strategies are available for the preparation of allenyl complexes [3]; some of us recently reported [3a] that the protonation of diiron-cyclopentenone complexes [4] bearing a OH-group in their side chain represented a straightforward route to

the formation of cationic μ-allenyl derivatives. The same procedure is viable for analogous diruthenium [3b] and mixed iron-ruthenium systems [5].

Herein we report that electrophilic additions to the (propen-2-yl)dimetallacyclopentenone complex $[Fe_2Cp_2(CO)(\mu\text{-}CO)\{\mu\text{-}\eta^1\text{:}\eta^3\text{-}C_\alpha(H)\text{=}C_\beta(C_\gamma(CH_3)CH_2)C(=O)\}]$ (**1**) [3a] result in the formation of μ-allenyl species. DFT calculations have been carried out in order to provide theoretical insights into the experimental results.

2. Results and discussion.

The complex $[Fe_2Cp_2(CO)(\mu\text{-}CO)\{\mu\text{-}\eta^1\text{:}\eta^3\text{-}C_\alpha(H)\text{=}C_\beta(C_\gamma(CH_3)CH_2)C(=O)\}]$ (**1**), in dichloromethane solution, reacted with electrophiles to give the μ-allenyl derivatives $[Fe_2Cp_2(CO)_2(\mu\text{-}CO)\{\mu\text{-}\eta^1\text{:}\eta^2{}_{\alpha,\beta}\text{-}C_\alpha H\text{=}C_\beta\text{=}C_\gamma(CH_3)(CH_2E)\}][BF_4]$ (E = CPh_3, [**2**][BF_4]; E = H, [**3**][BF_4]), Scheme 1. The products were isolated in high yields after work-up.

Scheme 1 about here

The formation of the allenyl compound $[\mathbf{2}]^+$ is the consequence of the selective C–C coupling of the $[CPh_3]^+$ cation with the propen-2-yl unit in **1** [6]. Compound [**2**][BF_4] was characterized by IR and NMR spectroscopy, elemental analysis and electrochemistry. Furthermore, X-ray quality crystals were collected from a CH_2Cl_2/Et_2O mixture at low temperature (see Experimental). The ORTEP molecular diagram of $[\mathbf{2}]^+$ is shown in Figure 1, with the relevant bond lengths and angles reported in Table 1. The structure of the $[\mathbf{2}]^+$ cation closely resembles those of other diiron and diruthenium μ-allenyl complexes previously reported [3a]. The cation is based on a *cis*-$[Fe_2(Cp)_2(CO)_2(\mu\text{-}CO)]$ core to which is coordinated the bridging $\{\mu\text{-}\eta^1\text{:}\eta^2\text{-}C(H)\text{=}C\text{=}C(Me)(CH_2CPh_3)\}$ allenyl ligand. The bonding parameters of the latter are as

expected for this class of ligands [7], with C(14)-C(15)-C(16) considerably bent [151.4(6)°; usual values are in the 143-157° range] and both C(14)-C(15) [1.362(9)] and C(15)-C(16) [1.311(9)] displaying considerable π-character [usual values are in the 1.36-1.40 and 1.31-1.35 Å ranges, respectively]. The bridging CO ligand is asymmetric with the shorter contact toward Fe(2), which is η^1-coordinated to the allenyl ligand.

Figure 1 and Table 1 about here

The IR spectrum of [**2**][BF_4] (in CH_2Cl_2 solution) displays clearly the absorptions due to terminal (at 2038 and 2013 cm^{-1}) and bridging carbonyls (1868 cm^{-1}), respectively.

The NMR spectra (in CD_3CN solution at 298 K) of the product isolated from the reaction of **1** with [CPh_3][BF_4] contain a single set of signals, indicating that the addition of the [CPh_3] group to **1** takes place with regio- and stereo-specificity. The ^{13}C spectrum displays the resonances due to the C_β and C_γ respectively at 154.2 and 123.0 ppm, in accordance with what has been reported for similar compounds [3a,b]. The [$C_\alpha H$] nuclei are seen in the high-frequency region [$\delta(^1H)$ = 9.83 ppm; $\delta(^{13}C)$ = 145.9 ppm]. The C_γ-*Me* group resonates at 1.57 ppm (^1H) and 24.4 ppm (^{13}C), respectively. It should be noted that the C_γ-bound methyl groups in the allenyl [$Fe_2Cp_2(CO)_2(\mu\text{-}CO)\{\mu\text{-}\eta^1\text{:}\eta^2{}_{\alpha,\beta}\text{-}C_\alpha H{=}C_\beta{=}C_\gamma(CH_3)_2\}$][$BF_4$] give raise to resonances at 2.28, 1.94 ppm (^1H) and 27.7, 23.2 ppm (^{13}C); the higher-field resonances [1.94 (^1H), 23.2 (^{13}C) ppm] were attributed to the methyl pointing towards the Fe–Fe axis [3a,b]. On account of this feature, it may be concluded that the cation [**2**]$^+$ in solution holds the C_γ-methyl pointing at the Fe–Fe axis, and thus the [CH_2CPh_3] moiety far from the same axis. This is the same configuration as that found in the solid state (see above).

Diiron and diruthenium allenyl complexes usually exhibit a fast exchange process at room temperature (σ-π fluxionality [3b], Scheme 2). The observance of clear ^{1}H and ^{13}C NMR spectra at room temperature lends support to the lack of fluxionality for $[\mathbf{2}]^{+}$; this is probably a consequence of the steric encumbrance exerted by the $[CH_2CPh_3]$ group.

Scheme 2 about here

Complex $[\mathbf{2}][BF_4]$ in $CH_2Cl_2/[N^nBu_4][PF_6]$ solution underwent one irreversible oxidation at +1.20 V (*vs* $FeCp_2$) and three consecutive reduction processes at −1.01, −1.99 and −2.30 V. Analysis of the cyclic voltammograms, with scan rates varying between 0.02 and 1.00 V s^{-1}, confirmed the electrochemically-reversible, diffusion-controlled nature of the first reduction, complicated by a subsequent chemical reaction (i_{pa}/i_{pc} = 0.73 at 1.0 V s^{-1}).

Former studies established that diruthenium μ-allenyl cations analogous to $[\mathbf{2}]^{+}$ could exist in two isomeric forms differing from each other in the orientation of the C_γ-substituents [3b]. On considering this fact, we optimized by DFT calculations the structures of the possible isomers for the cation $[Fe_2Cp_2(CO)_2(\mu\text{-}CO)\{\mu\text{-}\eta^1\text{:}\eta^2{}_{\alpha,\beta}\text{-}C_\alpha H{=}C_\beta{=}C(CH_3)(CH_2CPh_3)\}]^{+}$. The computed structures ($[\mathbf{2a}]^{+}$, $[\mathbf{2b}]^{+}$) are shown in Figure 2, and a selection of calculated geometric parameters is given in Table S1. The structure $[\mathbf{2a}]^{+}$ corresponds to the one found experimentally. A compared reading of Tables 1 and S1 outlines that the theoretical parameters are in good agreement with the X-ray data.

Figure 2 about here

According to the DFT calculations, the cation $[\mathbf{2a}]^+$ is more stable than the stereoisomer $[\mathbf{2b}]^+$ by about 7 kcal mol^{-1}. This result appears to be a consequence of the major steric hindrance exerted by the $[CH_2CPh_3]$ substituent with respect to [Me], and is in alignment with the experimental evidences (i.e. $[\mathbf{2b}]^+$ does not form).

The selective formation of $[\mathbf{3}]^+$ by reaction of **1** with $HBF_4 \cdot Et_2O$ deserves a detailed discussion. It was reported that the reaction of the dimetallacyclopentenone compound $[Fe_2Cp_2(CO)(\mu\text{-}CO)\{\mu\text{-}\eta^1\text{:}\eta^3\text{-}C_\alpha H{=}C_\beta(Ph)C(=O)\}]$ (**4**) with $HBF_4 \cdot Et_2O$ afforded readily the vinyl species $[Fe_2Cp_2(CO)_2(\mu\text{-}CO)\{\mu\text{-}\eta^1\text{:}\eta^2\text{-}C_\alpha H{=}C_\beta H(Ph)\}][BF_4]$ ($[\mathbf{5}][BF_4]$) via protonation at the C_β centre, see Introduction [4, 8]. Since compound **1** has a dimetallacyclopentenone core likewise **4**, at least two sites in the former might be susceptible to H^+ attack: *a*) the $[CH_2]$ fragment in the propen-2-yl unit; *b*) the C_β carbon. The observed formation of $[\mathbf{3}]^+$ is the consequence of proton addition at site *a*). Alternative addition at site *b*) would produce the hypothetical vinyl complex $[Fe_2Cp_2(CO)_2(\mu\text{-}CO)\{\mu\text{-}\eta^1\text{:}\eta^2\text{-}C_\alpha H{=}C_\beta HC_\gamma(Me){=}CH_2\}]^+$ ($[\mathbf{6}]^+$).

In the attempt to shed some light on the chemical behaviour of **1**, its electrochemical properties were studied by cyclic voltammetry. Compound **1** underwent one reduction process at −1.90 V and one oxidation at +0.08 V (*vs* $FeCp_2$, $CH_2Cl_2/[N^nBu_4][PF_6]$ solution). Analysis of the cyclic voltammograms, with scan rates varying between 0.02 and 1.00 V s^{-1}, confirmed the electrochemically-reversible, diffusion-controlled nature of the two processes. A fast chemical reaction followed the oxidation (i_{pc}/i_{pa} = 0.28 at 1.0 Vs^{-1}) and new, unidentified, redox active compounds formed as indicated by the appearance of two reduction processes (at −0.7 and −1.02 V). Also the reduction of **1** is a partially chemically reversible process (i_{pa}/i_{pc} = 0.40 at 1.0 Vs^{-1}).

The electrochemistry of **1** closely resembles that previously observed for **4** in CH_2Cl_2 solution [8b]. This fact suggests that the redox changes, in both complexes **1** and **4**, are negligibly affected by the nature of the C_β-substituent in the hydrocarbyl skeleton.

Thus, in order to rationalize the different reactivity with H^+ exhibited respectively by **1** and **4**, we optimized the structures of **1**, $[\mathbf{3}]^+$, **4**, $[\mathbf{5}]^+$ and $[\mathbf{6}]^+$ by DFT calculations, with the addition of an implicit solvation model for dichloromethane in the cases of $[\mathbf{3}]^+$ and $[\mathbf{6}]^+$. The computed structures, together with the corresponding salient geometric parameters, are given as Supplementary Information (Figures S1-S5 and Tables S2-S6). The geometric parameters calculated for $[\mathbf{3}]^+$ and **4** are strictly comparable with those previously obtained by single-crystal X-Ray diffractometry [3a, 8b], with deviations between computed and experimental bond lengths below 1%. The gas-phase proton affinities for the reactions $\{[\mathbf{5}]^+ \rightarrow \mathbf{4} + H^+\}$ and $\{[\mathbf{3}]^+ \rightarrow \mathbf{1} + H^+\}$ were determined to be respectively 237 and 238 kcal mol^{-1}. These values match well with those reported for organic bases such as 3,4,5-trimethylpyridine and 1,5-dimethylimidazole [9] and, being closely similar to each other, indicate a comparable basicity of the neutral complexes **4** and **1**.

Interestingly, the highest-energy occupied molecular orbitals of **1** are mainly localized on C_β and on the methylene carbon. The pattern of the Fukui's function $f_(r)$ [10] calculated for **1** (Figure 3) agrees in that both such carbon atoms are potential sites of electrophilic attack; indeed the function is localized on Fe1, C_β and, to lower extent, the $[CH_2]$ carbon.

Figure 3 about here

According to the calculations, compounds $[\mathbf{6}]^+$ and $[\mathbf{3}]^+$ have similar enthalpy values both in the gas-phase and in CH_2Cl_2 (ΔH is comprised between 1 and 2 kcal mol^{-1}). This fact

prompted us to find a route for the possible conversion of [**3**]$^+$ into its isomer [**6**]$^+$ via hydrogen intramolecular migration. Heating a solution of [**3**][BF_4] in acetonitrile at reflux temperature resulted in prevalent decomposition [compound $Fe_2Cp_2(CO)_4$ was recovered in ca. 25% yield], while analogous treatment in boiling $CHCl_3$ or $(CH_2Cl)_2$ solution was ineffective. The employment of small amounts of a potential catalyst such as $NHEt_2$ did not influence significantly the outcomes of these processes.

The reaction of **1** with $HBF_4 \cdot Et_2O$, affording [**3**]$^+$, is the reverse of the formation of **1** by deprotonation of [**3**][BF_4] [3a]. The synthetic sequence [**3**]$^+ \rightarrow$ **1** $\rightarrow$ [**2**]$^+$ represents a feasible route for the functionalization of the allenyl ligand, proceeding via C–H activation and C–C bond formation. The overall result involves the incorporation of the $[CPh_3]^+$ group with the displacement of the acidic proton from the methyl group of [**3**]$^+$. With the aim of obtaining a functionalized allenyl species by one-pot process, we allowed [**3**][BF_4] to react with $NHEt_2$ in the presence of PhSSPh. Indeed a similar strategy proved to be efficient for the displacement of one acidic hydrogen with the $[SPh]^+$ unit in diiron μ-vinyliminium complexes [11]. Nevertheless the reaction of [**3**][BF_4] with $NHEt_2$/PhSSPh failed to give the expected SPh-functionalized allenyl complex. Instead the previously reported mononuclear compound [$FeCp(CO)_2SPh$] (**7**) [12] was isolated in good yield.

The fragmentation reaction leading to **7** suggests that some mechanism including the formation of radical species could be operative. It has to be remarked that previous studies on [**3**]$^+$ have outlined that this complex can be easily monoelectronically reduced to a radical intermediate bearing most of the unpaired electron density on the iron centres [8b]. The capture of this metal-based radical by PhSSPh, acting as radical scavenger, may determine the breaking of the Fe–Fe bond and the consequent formation of **7**.

3. Conclusions

The reactions of a diiron propen-2-yl-dimetallacyclopentenone complex with electrophiles (H^+, CPh_3^+) result in straightforward synthesis of μ-allenyl derivatives. In particular, the protonation reaction represents the reverse of the formation of the propen-2-yl-dimetallacyclopentenone reactant by deprotonation of the allenyl product.

Therefore the allenyl ligand [$-C_\alpha=C_\beta=C_\gamma Me_2$], bridged coordinated to diiron frame, may be viewed as a feasible material for organic transformation, occurring via C–H bond activation and successive C–C formation. Otherwise treatment of such allenyl species with amine, in the presence of a potential radical scavenger (PhSSPh), leads to Fe–Fe cleavage and formation of a SPh-containing monoiron complex.

4. Experimental details

4.1. General

Reactions were carried out under nitrogen atmosphere, using standard Schlenk techniques. Glassware was oven-dried before use. Solvents were distilled before use under nitrogen from appropriate drying agents. Chromatography separations were carried out on columns of Alumina (Fluka, Brockmann Activity I) or Celite (Fluka, 512 Medium). All reactants were commercial products (Sigma-Aldrich) of the highest purity available and used as received. Compound **1** [3a] and ferrocene [13] were prepared according to the literature. Infrared spectra were recorded at 298 K on FT-IR Perkin–Elmer Spectrometer equipped with a UATR sampling accessory (solid samples). NMR measurements were performed at 298 K (unless otherwise stated) on Bruker Avance DRX400 instrument equipped with probe BBFO broadband. The chemical shifts for ^1H and ^{13}C NMR spectra were referenced to the non deuterated aliquot of the solvent; the spectra were fully assigned *via* DEPT experiments and ^1H,^{13}C correlation measured through gs-HSQC and gs-HMBC experiments [14].

Apparatus and techniques for the electrochemical measurements were previously described [7]. Electrochemical measurements were performed in 0.2 M CH_2Cl_2 solutions of $[N^nBu_4][PF_6]$ as supporting electrolyte and all potential values were referenced to the ferrocene/ferrocenium couple (ferrocene was added as internal reference).

Carbon and hydrogen analyses were performed on Carlo Erba mod. 1106 instrument.

The computational geometry optimization of the complexes was carried out using the hybrid DFT EDF2 method [15] without symmetry constraints, in combination with the LACVP** basis set, which is a combination of the 6-31G(d,p) basis set with the LANL2DZ effective core basis set [16].

Further refining was carried out for **1**, $[\mathbf{3}]^+$, **4**, $[\mathbf{5}]^+$ and $[\mathbf{6}]^+$ with the hybrid DFT M06 functional [17] in combination with a polarized triple-ζ quality basis set composed by the 6-311G(d,p) basis set on the light atoms and the LANL2TZ(f) basis set on the metal centre [18]. The "restricted" formalism was applied to all the complexes. The stationary points were characterized by IR simulations, from which the zero-point vibrational energies were computed. In every cases the Hessian afforded positive eigenvalues. The thermal contributions to enthalpy were calculated on the basis of statistical mechanics standard formulae (rigid-rotor approximation). Proton affinity values were calculated from computed quantities as reported in the literature [19]. Implicit solvation was added during the optimization of $[\mathbf{3}]^+$ and $[\mathbf{6}]^+$ by using the C-PCM model for dichloromethane [20]. The Fukui's function $f_-(r)$ for **1** was obtained from the electron density of this compound and from the electron density of the same compound missing of one electron [10]. DFT EDF2 calculations were carried out with Spartan 08 [21], while Gaussian 09 was used for the calculations based on the M06 functional [22]. All the calculations were performed on x86-64 workstation based on Intel Core I7 processor.

*4.2. Synthesis of [$Fe_2Cp_2(CO)_2(\mu\text{-}CO)\{\mu\text{-}\eta^1:\eta^2_{\alpha,\beta}\text{-}C_\alpha H{=}C_\beta{=}C(CH_3)(CH_2E)][BF_4]$ (E = CPh_3, [**2**][BF_4]; E = H, [**3**][BF_4]).*

A solution of complex **1** (0.300 g, 0.765 mmol) in CH_2Cl_2 (15 mL) was treated with [CPh_3][BF_4] (0.260 g, 0.788 mmol). The mixture was stirred at room temperature for 24 hours. Hence the volatile materials were removed in vacuo. The resulting residue was washed with Et_2O (2 x 20 mL), then dissolved in CH_2Cl_2 and filtered on a Celite pad. Removal of the solvent afforded a dark-red solid corresponding to [**2**][BF_4] (yield 0.497 g, 90%). Red crystals suitable for X-ray analysis were collected from a CH_2Cl_2 solution layered with Et_2O and stored at –30°C. Anal. Calcd. for $C_{37}H_{31}BF_4Fe_2O_3$: C, 61.54; H, 4.33. Found: C, 61.37; H, 4.48. IR (CH_2Cl_2): ν(CO) 2038(vs), 2013(m), 1868(m) cm^{-1}. ^1H NMR (CD_3CN) δ 9.83 (s, 1 H, $C_\alpha H$); 7.59-7.33 (15 H, Ph); 5.39, 5.09 (s, 10 H, Cp), 4.26, 3.61 (d, 2 H, $^2J_{HH}$ = 14 Hz, CH_2); 1.57 (s, 3 H, Me). $^{13}C\{^1H\}$ NMR (CD_3CN) δ 241.5 (μ-CO); 210.2, 206.0 (CO); 154.2 (C_β); 147.6 (ipso-Ph); 145.9 (C_α); 129.7, 128.4, 126.7 (Ph); 123.0 (C_γ); 92.3, 88.0 (Cp); 58.7 (*C*Ph_3); 50.4 (CH_2); 24.4 (Me).

The reaction of **1** (0.450 mmol) with $HBF_4{\cdot}Et_2O$ (0.460 mmol) was carried out by the same procedure as that described for the synthesis of [**2**][BF_4]. Thus complex [**3**][BF_4] was recovered in 85% yield.

*4.3. Thermal stability of [$Fe_2Cp_2(CO)_2(\mu\text{-}CO)\{\mu\text{-}\eta^1:\eta^2_{\alpha,\beta}\text{-}C_\alpha H{=}C_\beta{=}C(CH_3)_2][BF_4]$ ([**3**][BF_4]).*

Compound [**3**][BF_4] (0.300 g, 0.625 mmol) was dissolved in the appropriate solvent (10 mL) and heated at reflux temperature for 18 hours. Then the mixture was allowed to cool to room temperature and filtered through a celite pad. The filtered solution was dried in vacuo, then the resulting residue was dissolved in CD_2Cl_2 (0.5 mL) and analyzed by NMR at –40°C.

a) solvent = $CHCl_3$. NMR analysis: [**3**][BF_4];

b) solvent = CH_3CN. NMR analysis: prevalent $Fe_2Cp_2(CO)_4$, in admixture with non identified products;

c) solvent = $(CH_2Cl)_2$. NMR analysis: [**3**][BF_4], $Fe_2Cp_2(CO)_4$ and non identified products;

d) solvent = $(CH_2Cl)_2$/$NHEt_2$ (0.063 mmol). NMR analysis: [**3**][BF_4], $Fe_2Cp_2(CO)_4$ and non identified products.

*4.4. Reaction of [$Fe_2Cp_2(CO)_2(\mu$-CO)$\{\mu$-η^1:$\eta^2_{\alpha,\beta}$-$C_\alpha H$=C_β=$C(CH_3)_2$][BF_4] ([**3**][BF_4]) with $PhSSPh/NHEt_2$. Synthesis of [$FeCp(CO)_2SPh$] (**7**) [12].*

A solution of complex [**3**][BF_4] (0.450 g, 0.938 mmol) in CH_2Cl_2 (20 mL) was treated with PhSSPh (3.05 mmol) and then with $NHEt_2$ (10.0 mmol). The mixture was stirred at room temperature for 24 hours. Hence some alumina was added to the mixture, and the volatile materials were removed under vacuo. The solid residue was charged on alumina pad previously treated with water (6% H_2O *p/p*). A brown-red band was collected by using hexane/Et_2O (1:1 *v/v*) as eluent. Compound **7** was obtained as a powder upon removal of the volatile materials (yield 0.201 g, 75%). IR (CH_2Cl_2): ν(CO) 2032(s), 1984(vs) cm^{-1}. ^1H NMR ($CDCl_3$) δ 7.55-7.13 (5 H, Ph); 4.96 (s, 5 H, Cp). $^{13}C\{^1H\}$ NMR (CD_2Cl_2) δ 213.2 (CO); 143.3, 135.1, 128.2, 124.8 (Ph); 85.5 (Cp).

*4.5. X-ray characterization of [$Fe_2Cp_2(CO)_2(\mu$-CO)$\{\mu$-η^1:$\eta^2_{\alpha,\beta}$-$C_\alpha H$=C_β=$C(CH_3)(CH_2CPh_3)$}][BF_4] ([**2**][BF_4]).*

Crystal data and collection details for [**2**][BF_4] are reported in Table 2. The diffraction experiment was carried out on Bruker Apex II diffractometer equipped with a CCD detector using Mo-Kα radiation. Data were corrected for Lorentz polarization and absorption effects

(empirical absorption correction SADABS) [23]. The structure was solved by direct method and refined by full-matrix least-squares based on all data using F^2 [24]. All non-hydrogen atoms were refined with anisotropic displacement parameters. H-atoms were placed in calculated positions, except H(14) which was located in the Fourier map and the C(14)-H(14) distance restrained to 0.96 Å (s.u. 0.02) during refinement. H-atoms were treated isotropically using the 1.2 fold U_{iso} value of the parent C-atoms, except methyl protons, which were assigned the 1.5 fold U_{iso} value of the parent C-atom. Similar U restraints (s.u. 0.01) were applied to the C and O atoms.

Table 2 about here

Acknowledgement

We thank the Ministero dell'Università e della Ricerca Scientifica e Tecnologica (MIUR) for financial support.

Supplementary Material

Figures S1-S5 report the DFT-calculated structures of **1**, [**3**]$^+$, **4**, [**5**]$^+$, [**6**]$^+$, respectively. Tables S1-S6 give selected calculated distances (Å) and angles (°) for [**2a**]$^+$/[**2b**]$^+$, **1**, [**3**]$^+$, **4**, [**5**]$^+$, [**6**]$^+$, respectively. Crystallographic data for [**2**][BF_4] have been deposited with the Cambridge Crystallographic Data Centre (CCDC 905444). Copies of this information can be obtained free of charge from the Director, CCDC, 12 Union Road, Cambridge CB2 1EZ, UK (fax: +44-1233-336033; deposit@ccdc.cam.ac.uk or www.ccdc.cam.ac.uk).

References

[1] (a) F. W. Patureau, S. de Boer, M. Kuil, J. Meeuwissen, P.-A. R. Breuil, M. A. Siegler, A. L. Spek, A. J. Sandee, B. de Bruin, J. N. H. Reek, J. Am. Chem. Soc. 131 (2009) 6683;
(b) C. T. Saouma, P. Müller, J. C. Peters, J. Am. Chem. Soc. 131 (2009) 10358;
(c) A. J. Esswein, A. S. Veige, P. M. B. Piccoli, A. J. Schultz, D. G. Nocera, Organometallics 27 (2008) 1073;
(d) V. Ritleng, M J. Chetcuti, Chem. Rev. 107 (2007) 797;
(e) J. R. Wigginton, A. Chokshi, T. W. Graham, R. McDonald, M. J. Ferguson, M. Cowie, Organometallics 24 (2005) 6398;
(f) R. D. Adams, B. Captain, J. Organomet. Chem. 689 (2004) 4521;
(g) K. Severin, Chem. Eur. J. 8 (2002) 1515.

[2] (a) R. Mazzoni, M. Salmi, V. Zanotti, Chem. Eur. J. 18 (2012) 10174;
(b) M. A. Alvarez, M. E. García, R. Gonzales, M. A. Ruiz, Dalton Trans. 42 (2012) 14498;
(c) M. A. Alvarez, M. E. García, R. González, M. A. Ruiz, Organometallics 29 (2010) 5140.
(d) F. Marchetti, S. Zacchini, M. Salmi, L. Busetto, V. Zanotti, Eur. J. Inorg. Chem. (2011) 1260;
(e) L. Busetto, F. Marchetti, F. Renili, S. Zacchini, V. Zanotti, Organometallics 29 (2010) 1797;
(f) L. Busetto, F. Marchetti, S. Zacchini, V. Zanotti, Organometallics 27 (2008) 5058;
(g) L. Busetto, F. Marchetti, S. Zacchini, V. Zanotti, Organometallics 26 (2007) 3577;
(h) V. G. Albano, L. Busetto, F. Marchetti, M. Monari, S. Zacchini, V. Zanotti, Organometallics 26 (2007) 3448.

[3] (a) A. Boni, F. Marchetti, G. Pampaloni, S. Zacchini, Dalton Trans. 39 (2010) 10866;
(b) S. A. R. Knox, F. Marchetti, J. Organomet. Chem. 692 (2007) 4119;
(c) G. Gervasio, D. Marabello, E. Sappa, A. Secco, J. Organomet. Chem. 690 (2005) 3755;
(d) S. Doherty, G. Hogarth, M. Waugh, W. Clegg, M. R. J. Elsegood, Organometallics 19 (2000) 5696;
(e) R. R. Willis, M. Calligaris, P. Faleschini, A. Wojcicki, J. Cluster Sci., 11 (2000) 233;

(f) S. Doherty, M. R. J. Elsegood, W. Clegg, M. F. Ward, M. Waugh, Organometallics 16 (1997) 4251.

[4] A. F. Dyke, S. A. R. Knox, P. J. Naish, G. E. Taylor, J. Chem. Soc. Dalton Trans. (1982) 1297.

[5] J. N. L. Dennett, S. A. R. Knox, K. M. Anderson, J. P. H. Charmant, A. G. Orpen, Dalton Trans. (2005) 63.

[6] The reaction of **1** (0.400 mmol) with Ph_3CCl (2.00 mmol) afforded a dark-red solid presumably corresponding to [**3**][Cl]. Anal. Calcd. for $C_{37}H_{31}ClFe_2O_3$: C, 66.25; H, 4.66; Cl, 5.29. Found: C, 66.02; H, 4.80; Cl, 5.07. IR (CH_2Cl_2): ν(CO) 2038(vs), 2013(m), 1868(m) cm^{-1}.

[7] A. Wojcicki, Inorg. Chem. Commun., 5 (2002) 82.

[8] (a) A. F. Dyke, S. A. R. Knox, M. J. Morris, P. J. Naish, J. Chem. Soc. Dalton Trans. (1983) 1417.

(b) A. Boni, T. Funaioli, F. Marchetti, G. Pampaloni, C. Pinzino, S. Zacchini, J. Organomet. Chem., 696 (2011) 3551.

[9] (a) M. Bortoluzzi, G. Paolucci, G. Annibale, B. Pitteri, Polyhedron 28 (2009) 1079.

(b) M. Bortoluzzi, G. Paolucci, B. Pitteri, Polyhedron 29 (2010) 767.

[10] F. Jensen, Introduction to Computational Chemistry, 2nd ed., Wiley and Sons Ed., Chichester, 2007.

[11] L. Busetto, F. Marchetti, R. Mazzoni, M. Salmi, S. Zacchini, V. Zanotti, J. Organomet. Chem. 693 (2008) 3191.

[12] M. Ahmad, R. Bruce, G. R. Knox, J. Organomet. Chem., 6 (1966) 1.

[13] G. Wilkinson, Org. Synth. 36 (1956) 31.

[14] W. Willker, D. Leibfritz, R. Kerssebaum, W. Bermel, Magn. Reson. Chem. 31 (1993) 287.

[15] C.Y. Lin, M.W. George, P.M.W. Gill, Aust. J. Chem. 57 (2004) 365.

[16] (a) W. J. Hehre, R. Ditchfield, J. A. Pople, J. Chem. Phys. 56 (1972) 2257.

(b) P. J. Hay, W. R. Wadt, J. Chem. Phys. 82 (1985) 270.

(c) P. J. Hay, W. R. Wadt, J. Chem. Phys. 82 (1985) 299.

(d) M. Dolg, in: J. Grotendorst (Ed.), Modern Methods and Algorithms of Quantum Chemistry, vol. 1, John Neumann Institute for Computing, NIC Series, Jülich, 2000, pp. 479 – 508

[17] Y. Zhao, D. G. Truhlar, Theor. Chem. Acc. 120 (2008) 215.

[18] (a) A. D. McLean, G. S. Chandler, J. Chem. Phys. 72 (1980) 5639.
(b) L. E. Roy, P. J. Hay, R. L. Martin, J. Chem. Theory Comput. 4 (2008) 1029

[19] A. El Hammadi, M. El Mouhtadi, J. Mol. Struct. (THEOCHEM) 497 (2000) 241.

[20] (a) V. Barone, M. Cossi, J. Phys. Chem. A 102 (1998) 1995. (b) M. Cossi, N. Rega, G. Scalmani, V. Barone, J. Comput. Chem. (2003) 669

[21] Spartan 08, Version 1.1.1, Wavefunction, Inc., Irvine, CA, 2009. Except for molecular mechanics and semi-empirical models, the calculation methods used in Spartan have been documented in Y. Shao et al., Phys. Chem. Chem. Phys. 8 (2006) 3172. A discussion and assessment of commonly-used calculation methods is found in W. J. Hehre, A Guide to Molecular Mechanics and Quantum Chemical Calculations, Wavefunction, Inc., Irvine, CA, 2003.

[22] M. J. Frisch et al., Gaussian 09, revision C.01, Gaussian, Inc., Wallingford CT, 2010.

[23] G. M. Sheldrick, SADABS, Program for Empirical Absorption Correction, University of Göttingen, Germany, 1996.

[24] G. M. Sheldrick, SHELX97-Program for the refinement of Crystal Structure, University of Göttingen, Germany, 1997.

SCHEME 1

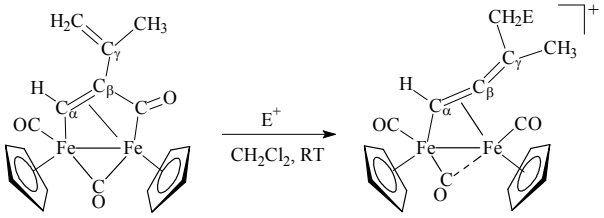

1

[**2**]$^+$ E = CPh_3

[**3**]$^+$ E = H

SCHEME 2

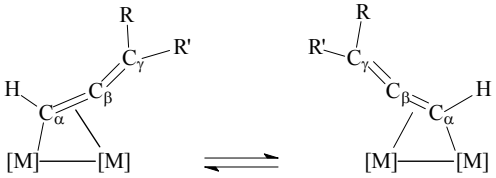

M = Fe or Ru
R, R' = H, alkyl or Ph

Captions for Tables and Figures

Table 1 Selected bond lengths (Å) and angles (°) for $[\mathbf{2}]^+$.

Table 2 Crystal data and experimental details for $[\mathbf{2}][BF_4]$.

Figure 1 Molecular structure of $[Fe_2Cp_2(CO)_2(\mu\text{-}CO)\{\mu\text{-}\eta^1\text{:}\eta^2{}_{\alpha,\beta}\text{-}C_\alpha H{=}C_\beta{=}C_\gamma(CH_3)(CH_2CPh_3)\}]^+$ ($[\mathbf{2}]^+$), with key atoms labelled. Thermal ellipsoids are at the 30% probability level. Only the main image of the disordered Cp bound to Fe(2) is drawn.

Figure 2 DFT-optimized structures of $[\mathbf{2a}]^+$ and $[\mathbf{2b}]^+$. Hydrogen atoms on Cp and Ph rings have been omitted for clarity.

Figure 3 Plot of the Fukui's function $f_-(r)$ for complex **1**. A coloured version of this image is available in the Supplementary Materials (Figure S1b).

TABLE 1

Fe(1)–Fe(2)	2.5953(12)	C(11)–O(3)	1.161(9)
C(11)–Fe(1)	2.112(7)	C(12)–O(1)	1.128(9)
C(11)–Fe(2)	1.843(7)	C(13)–O(2)	1.118(9)
C(12)–Fe(1)	1.769(8)	C(14)–C(15)	1.362(9)
C(13)–Fe(2)	1.785(8)	C(15)–C(16)	1.311(9)
C(14)–Fe(1)	2.032(6)	C(16)–C(17)	1.497(9)
C(14)–Fe(2)	1.950(7)	C(16)–C(18)	1.549(8)
C(15)–Fe(1)	2.087(7)	C(18)–C(19)	1.562(9)

Fe(2)–C(11)–Fe(1)	81.7(3)	Fe(2)–C(14)–Fe(1)	81.3(2)
C(15)–C(14)–Fe(2)	125.2(5)	C(16)–C(15)–C(14)	151.4(6)
C(15)–C(16)–C(17)	125.3(6)	C(15)–C(16)–C(18)	116.1(5)
C(17)–C(16)–C(18)	118.6(5)	C(16)–C(18)–C(19)	115.3(5)

TABLE 2

Formula	$C_{37}H_{31}BF_4Fe_2O_3$
Fw	722.13
T, K	291(2)
λ, Å	0.71073
Crystal system	Monoclinic
Space group	*Pc*
a, Å	10.538(2)
b, Å	9.089(2)
c, Å	17.114(7)
β, °	99.800(3)
Cell volume, Å^3	1615.5(6)
Z	2
D_c, g cm^{-3}	1.485
μ, mm^{-1}	0.985
F(000)	740
Crystal size, mm	0.16×0.17×0.11
θ limits, °	1.96-25.03
Reflections collected	14746
Independent reflections	5707 (R_{int} = 0.0694)
Data/restraints/parameters	5707 / 255 / 427
Goodness on fit on F^2	1.043
R_1 [$I > 2\sigma(I)$]	0.0655
wR_2 (all data)	0.1692
Largest diff. peak and hole, e.Å^{-3}	0.959 / –0.693

FIGURE 1

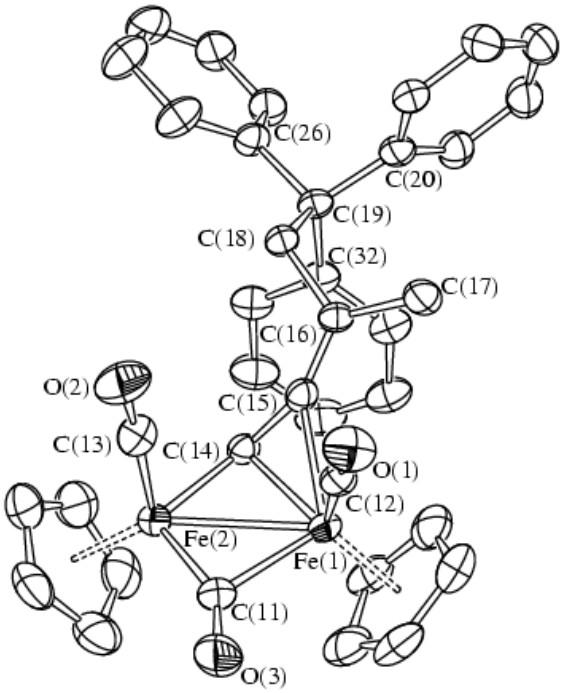

FIGURE 2

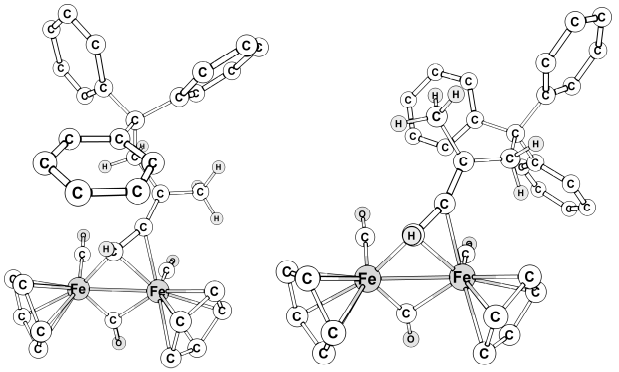

$[2a]^+$ $[2b]^+$

FIGURE 3